Regularized Energy Minimization Models in Image Processing

Tibor Lukić

Faculty of Technical Sciences,

University of Novi Sad, Serbia

SSIP Szeged, 2016

NOVI SAD

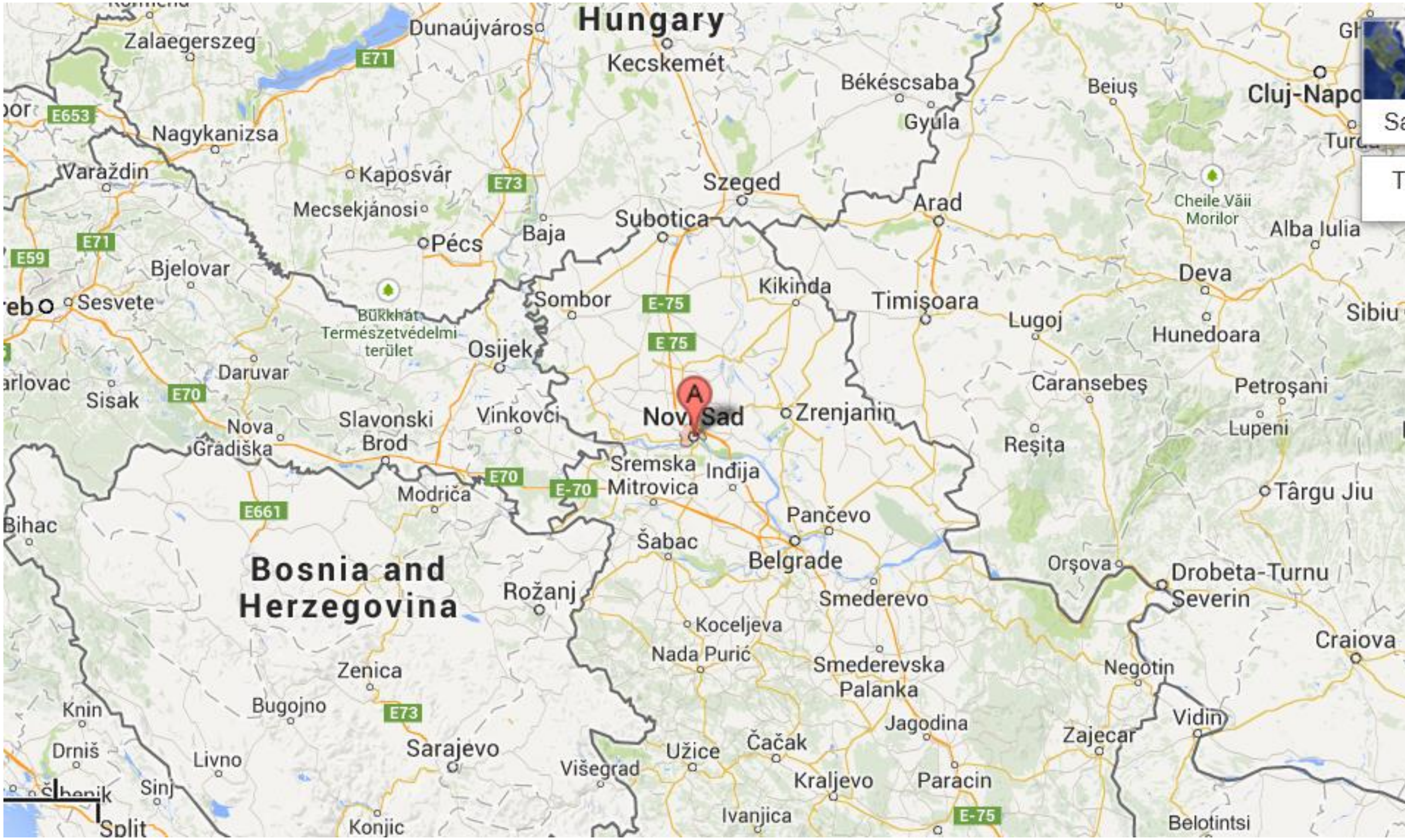

Hungary
Dunaújváros
Kecskemét
Zalaegerszeg
Békéscsaba
Beiuș
Cluj-Napo
Gyula
Nagykanizsa
Varaždin
Kaposvár
Szeged
Arad
Mecsekjánosi
Subotica
Baja
Pécs
Cheile Văii Morilor
Alba Iulia
Bjelovar
Sombor
Kikinda
Deva
Sesvete
Bükkhát Természetvédelmi terület
Timișoara
Lugoj
Hunedoara
Sibiu
Osijek
Daruvar
Caransebeș
Petroșani
Sisak
Vinkovci
Novi Sad
Zrenjanin
Slavonski Brod
Nova Gradiška
Reșița
Lupeni
Sremska Mitrovica
Inđija
Modriča
Târgu Jiu
Bihac
Pančevo
Šabac
Belgrade
Orșova
Drobeta-Turnu Severin
Bosnia and Herzegovina
Rožanj
Smederevo
Koceljeva
Craiova
Nada Purić
Smederevska Palanka
Negotin
Zenica
Knin
Bugojno
Jagodina
Vidin
Drniš
Sarajevo
Čačak
Zajecar
Livno
Sinj
Višegrad
Užice
Kraljevo
Paracin
Split
Konjic
Ivanjica
Belotintsi
E71
E653
E73
E59
E70
E-75
E 75
E661
E-70

SSIP 2017 WILL BE ORGANIZED IN **NOVI SAD**,

WELCOME!

NOVI SAD

NOVI SAD

UNIVERSITY OF NOVI SAD

UNS campus

Faculty of Technical Sciences

1200 employee

2500 first year students

OUTLINE

ENERGY-MINIMIZATION METHODS

REGULARIZED PROBLEMS

IMAGE DENOISING

DISCRETE TOMOGRAPHY

DESCRIPTORS

ENERGY-MINIMIZATION METHODS

Denoising example

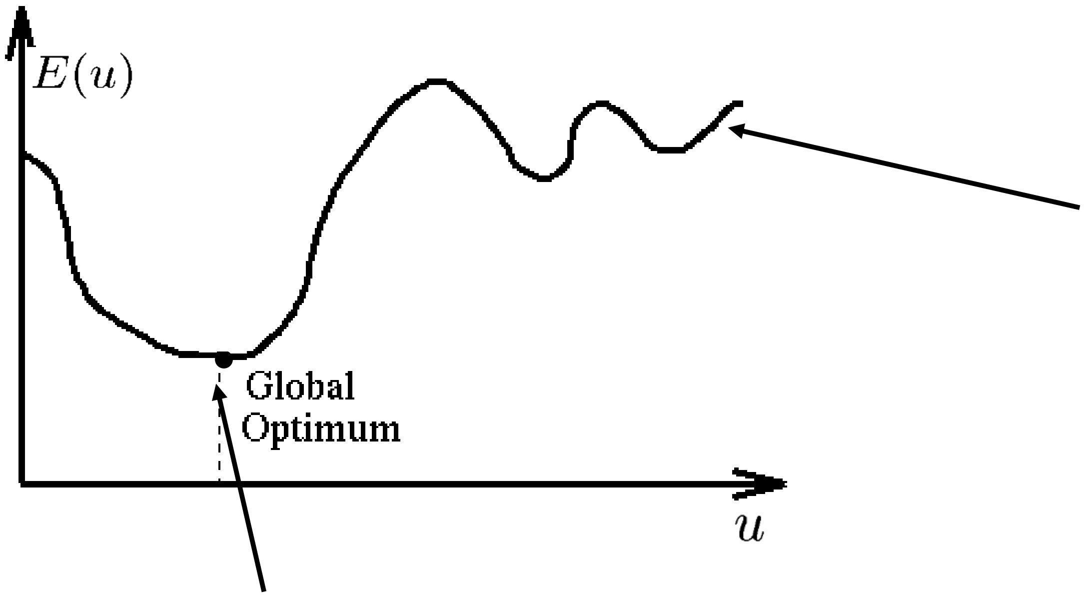

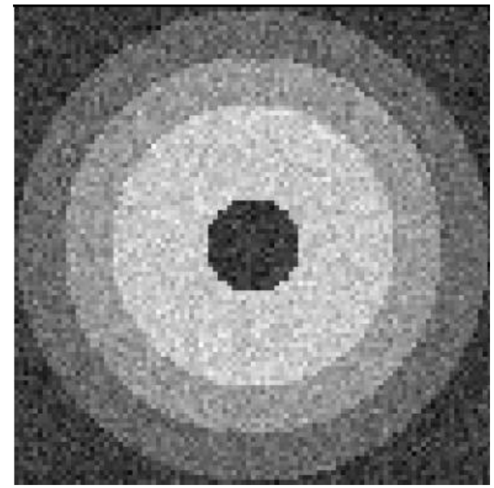

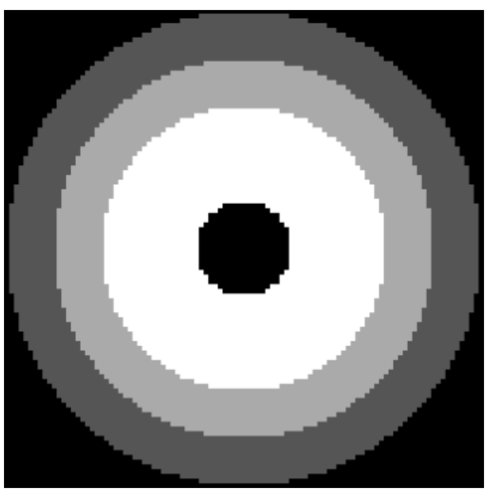

* Model design: $\min_u E(u)$

* Minimization process

REGULARIZED ENERGY FUNCTION

Regularized energy function

$$E(u) = \frac{\lambda}{2}\|Au - b\|^2 + \Psi(u)$$

data fitting term

regularization term

$\lambda > 0$ - balancing parameter, A - linear operator

b - observed data

Applications: denoising, deblurring, discrete tomography, classification, zooming, inpainting, stereo vision..

REGULARIZED ENERGY FUNCTION

$$f(x) = \frac{1}{2}||Ax - b||^2$$

Quadratic function, convex, but often not strictly convex.

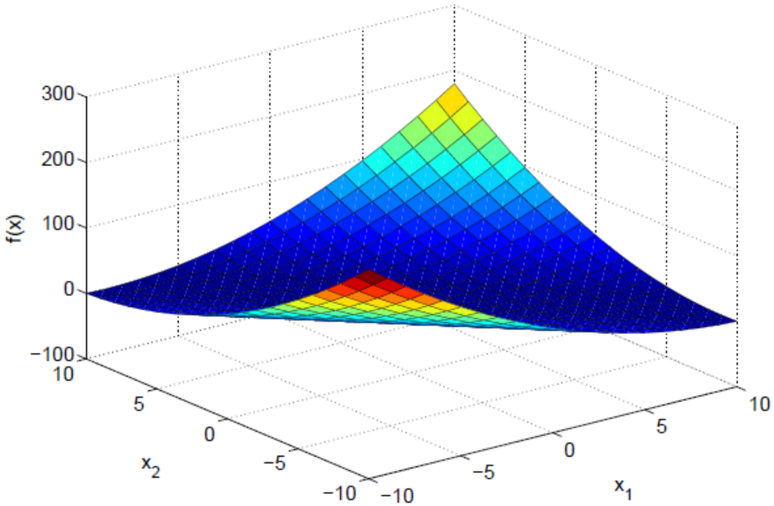

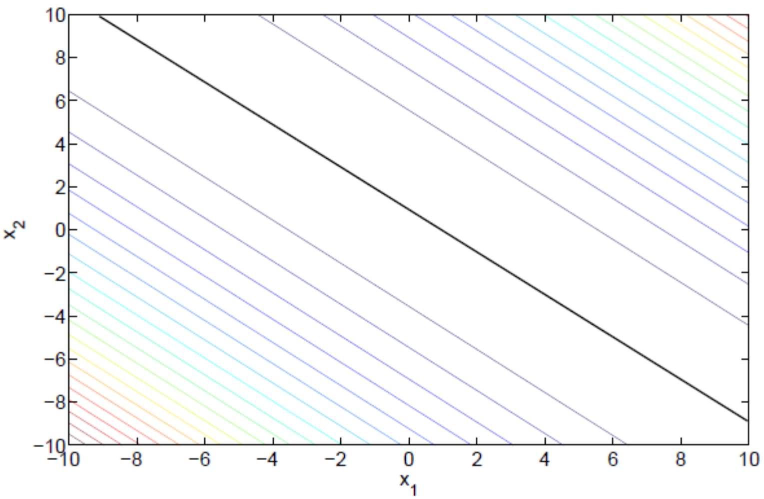

REGULARIZED ENERGY FUNCTION

$$E(u) = \frac{\lambda}{2}\|Au - b\|^2 + \Psi(u)$$

Example. Rudin et al. (1992) introduce the *Total variation* based regularization for denoising problem, where

$$\Psi(u) = \sum_{i=1}^{N} \|\nabla(u_i)\|.$$

REGULARIZED ENERGY FUNCTION

Discrete gradient

$$\nabla(u_i) = [u_r - u_i, u_b - u_i]^T$$

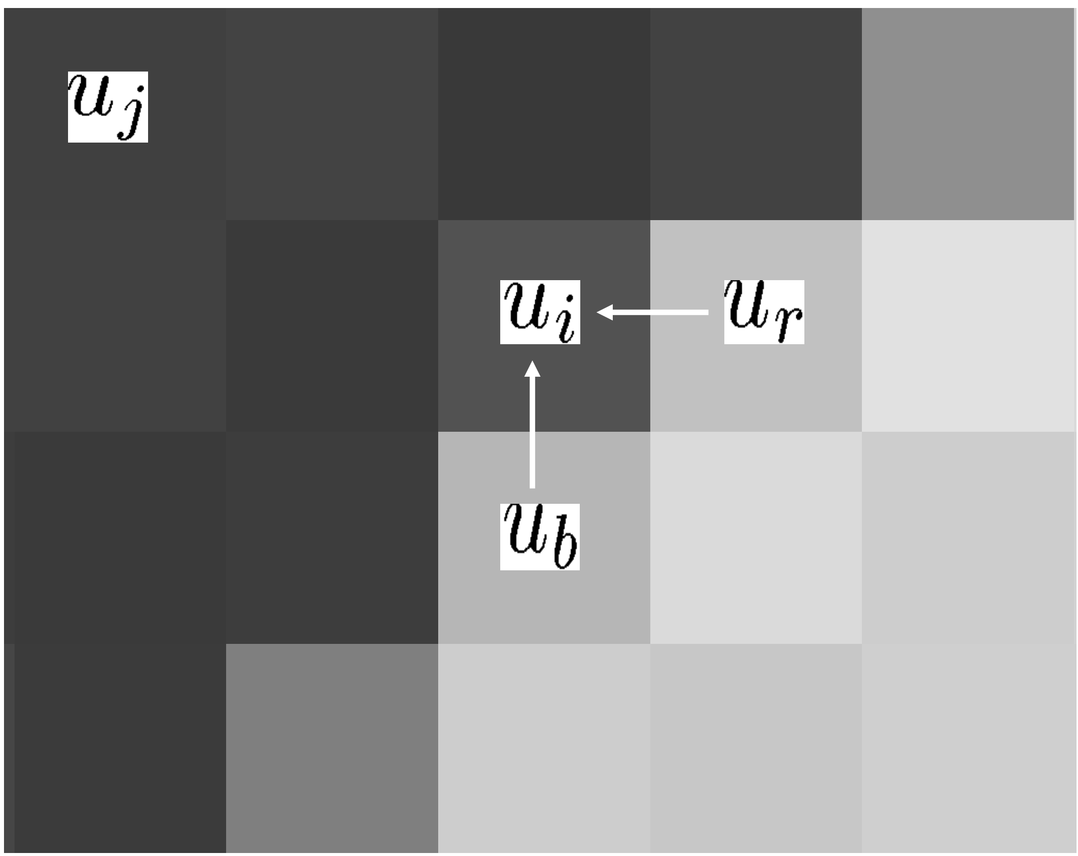

$$||\nabla(u_j)|| \leq ||\nabla(u_i)||$$

WHY WE USE THE GRADIENT?

In continuous case, we can consider the directional derivative:

$$\frac{\partial u}{\partial \vec{l}} = \nabla u \cdot \vec{l} = ||\nabla u|| \cdot ||\vec{l}|| \cdot \cos \sphericalangle(\nabla u, \vec{l}), \quad ||\vec{l}|| = 1$$

$$\max_{\vec{l}} \left| \frac{\partial u}{\partial \vec{l}} \right| = ||\nabla u||$$

IMAGE DENOISING

Noise clearly visible in an image from a digital camera.

Wikipedia

IMAGE DENOISING

Image noise is random (not present in the object imaged) variation of brightness or color information in images.

Random variation in the number of photons reaching the surface of the image sensor at same exposure level may cause noise *(**photon noise**).*

Incorrect lens adjustment or motion during the image acquisition may cause *blur*.

IMAGE DENOISING

The degradation model is given by

$$b = u^* + \omega \quad .$$

Regularized energy-minimization model:

$$\min_u \left(\frac{\lambda}{2} ||u - b||^2 + \sum_{i=1}^{N} \varphi(||\nabla u_i||) \right)$$

Minimization has several challenges:

large-scale problem, the objective function is non-differentiable at points where $||\nabla(u_i)|| = 0$, and it is convex only when φ is convex.

POTENTIAL FUNCTIONS

$\varphi(t)$	conve
total variation pot. fun.	
$\varphi 1(t) = t,$	yes
smoothing pot. fun.	
$\varphi 2(t) = t^\alpha,\ 1 < \alpha < 2$	yes
$\varphi 3(t) = t^2,$	yes
edge preserving pot. fun.	
$\varphi 4(t) = \begin{cases} t^2, & t \leq \alpha \\ 2\alpha t - \alpha^2, & t > \alpha \end{cases} \quad \alpha > 0$	yes
$\varphi 5(t) = \sqrt{\alpha + t^2},\ \alpha > 0$	yes
$\varphi 6(t) = \ln\cosh(\alpha t),\ \alpha > 0$	yes
$\varphi 7(t) = \dfrac{\alpha t^2}{1 + \alpha t^2},\ \alpha > 0$	no
$\varphi 8(t) = \ln(1 + \alpha t^2),\ \alpha > 0$	no
$\varphi 9(t) = 1 - e^{-\alpha t^2},\ \alpha > 0$	no
$\varphi 10(t) = \begin{cases} \sin(\alpha t^2), & 0 \leq t \leq \sqrt{\frac{\pi}{2\alpha}} \\ 1, & t > \sqrt{\frac{\pi}{2\alpha}} \end{cases} \quad \alpha > 0$	no

POTENTIAL FUNCTIONS

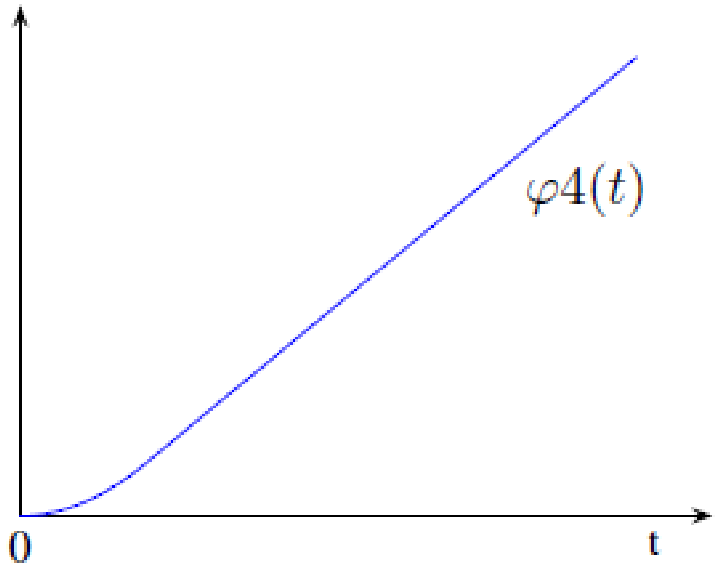

Huber potential

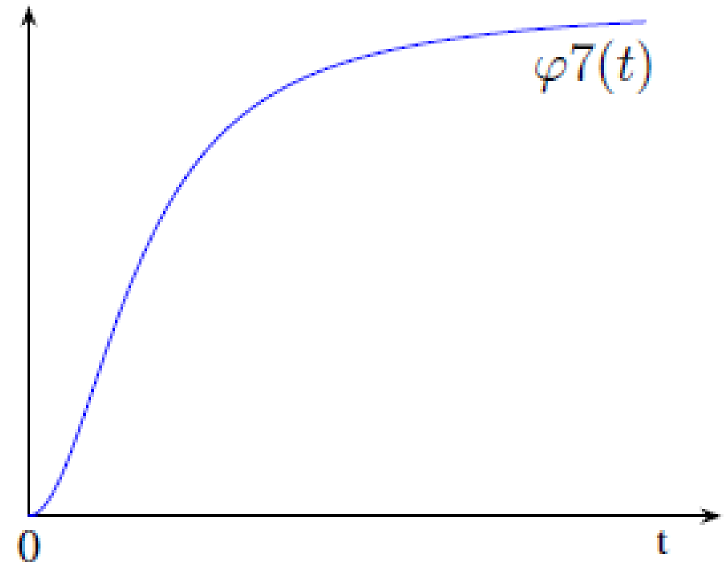

Geman & McClure potential

for high noise

for low noise

Several algorithms have proposed:

- Projection algorithm (PRO), Chambolle (2004), for TV only,
- Primal-Dual Hybrid Gradient (PDHG), Zhu and Chan (2008), for TV only,
- Fast Total Variation de-convolution (FTVd), Wang et al. (2008), for TV only,
- Spectral Gradient Based Optimization, Lukic et al. (2011),
- Elongation based image denoising model, Lukic and Zunic (2014).

IMAGE DENOISING

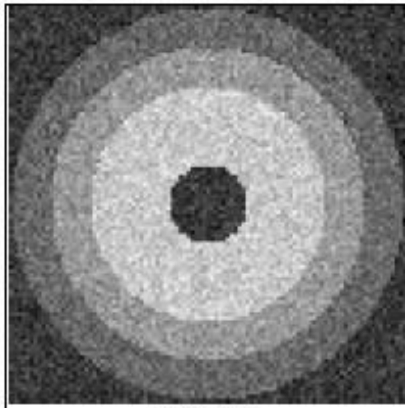	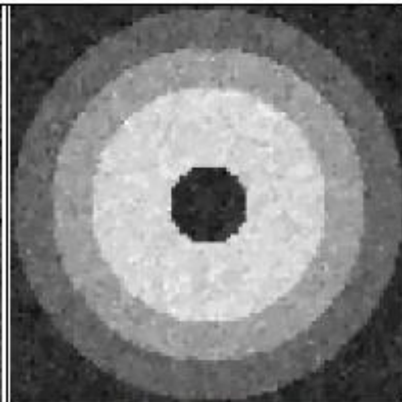	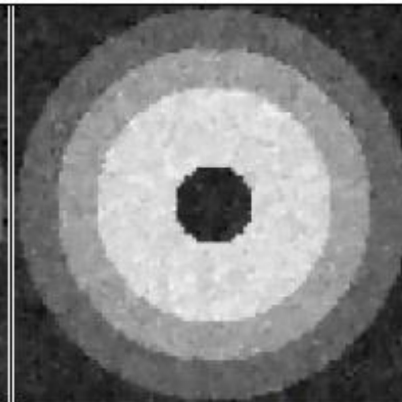	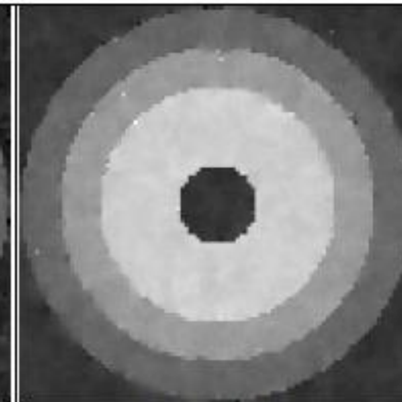
10dB	15.43dB	16.58dB	**19.08dB**
			
10dB	15.68dB	**16.57dB**	16.37dB
noisy image	$\varphi 1$ (TV)	$\varphi 4$	$\varphi 7$

Signal to Noise Ratio (dB): $\mathrm{SNR} = 10 * \log_{10} \dfrac{\|u^* - \widetilde{u}^*\|^2}{\|u^* - u^r\|^2}$.

DISCRETE TOMOGRAPHY

Tomography deals with the reconstruction of images, or slices of 3D volumes, from a number of projections obtained by penetrating waves through the considered object.

Applications in radiology, industry, materials science etc.

CT scanner

DISCRETE TOMOGRAPHY

Tomography deals with the reconstruction of images from a number of projections.

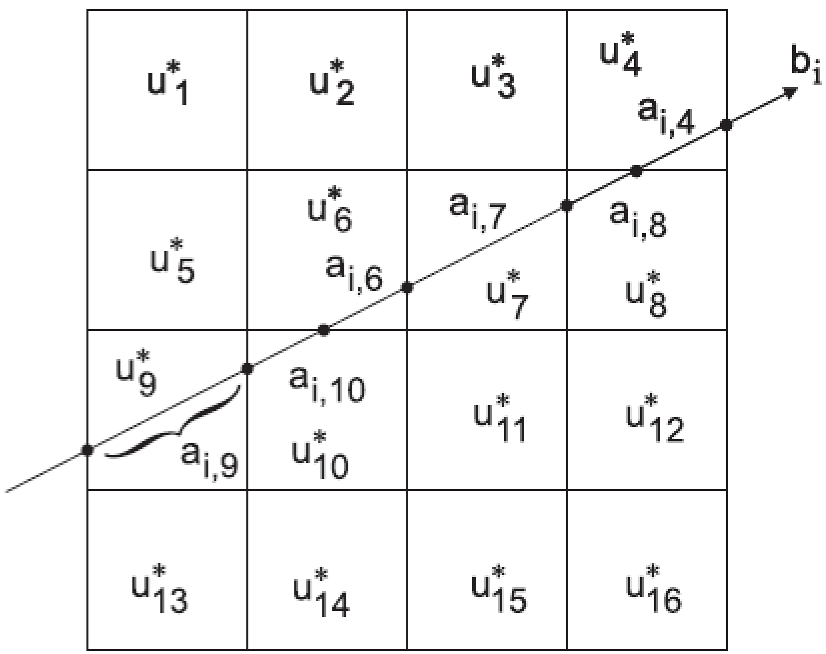

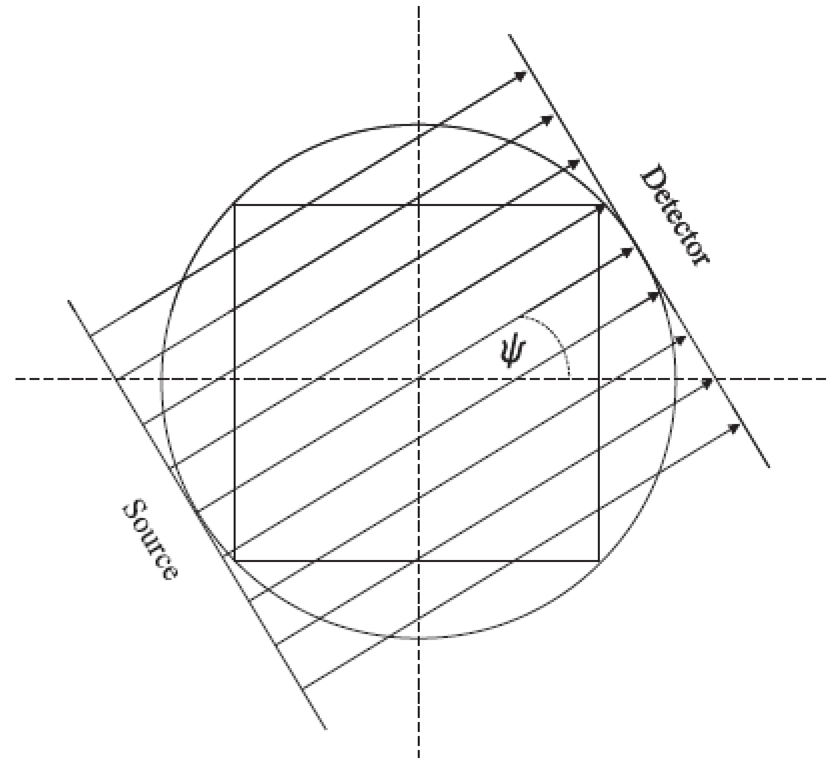

$$b_i = a_{i,4}u_4^* + a_{i,6}u_6^* + a_{i,7}u_7^* + a_{i,8}u_8^* + a_{i,9}u_9^* + a_{i,10}u_{10}^*$$

Reconstruction problem: $Au = b$, where the projection matrix $A \in \mathbb{R}^{M \times N}$ and vector $b \in \mathbb{R}^M$ are given.

DISCRETE TOMOGRAPHY

DT deals with reconstructions of images that contain a small number of gray levels from a number of projections:

$$u \in \{\mu_1, \mu_2, \ldots, \mu_k\}^N, \quad k \geq 2.$$

Main issue in DT: how to provide good quality reconstructions from as small number of projections as possible.

DT reconstruction problem can be formulated as a constrained minimization problem:

$$\min_{u \in \Lambda^N} E_{DT}(u;\lambda) := \frac{1}{2}\|Au - b\|^2 + \frac{\lambda}{2}\sum_{i=1}^{N}\|\nabla(u_i)\|^2,$$

where $\Lambda = \{\mu_1, \mu_2, \ldots, \mu_k\}$.

For binary tomography, Schüle et al. (2005) introduce the *convex-concave regularization:*

$$\min_{u \in [0,1]^N} \left(E_{DT}(u;\lambda) + \mu \left\langle u, \tau - u \right\rangle \right) , \quad \mu > 0$$

where $\tau = [1, 1, \ldots, 1]^T$.

In general case:

$$\min_{u} \; E_{DTW}(u;\lambda,\rho) := E_{DT}(u;\lambda) + \rho \sum_{i=1}^{N} W(u_i) , \quad \lambda, \rho > 0$$

where W is a *multi-well potential* function. The proposed energy, E_{DTW} is differentiable and quadratic.

Construction of the *multi-well potential* function.

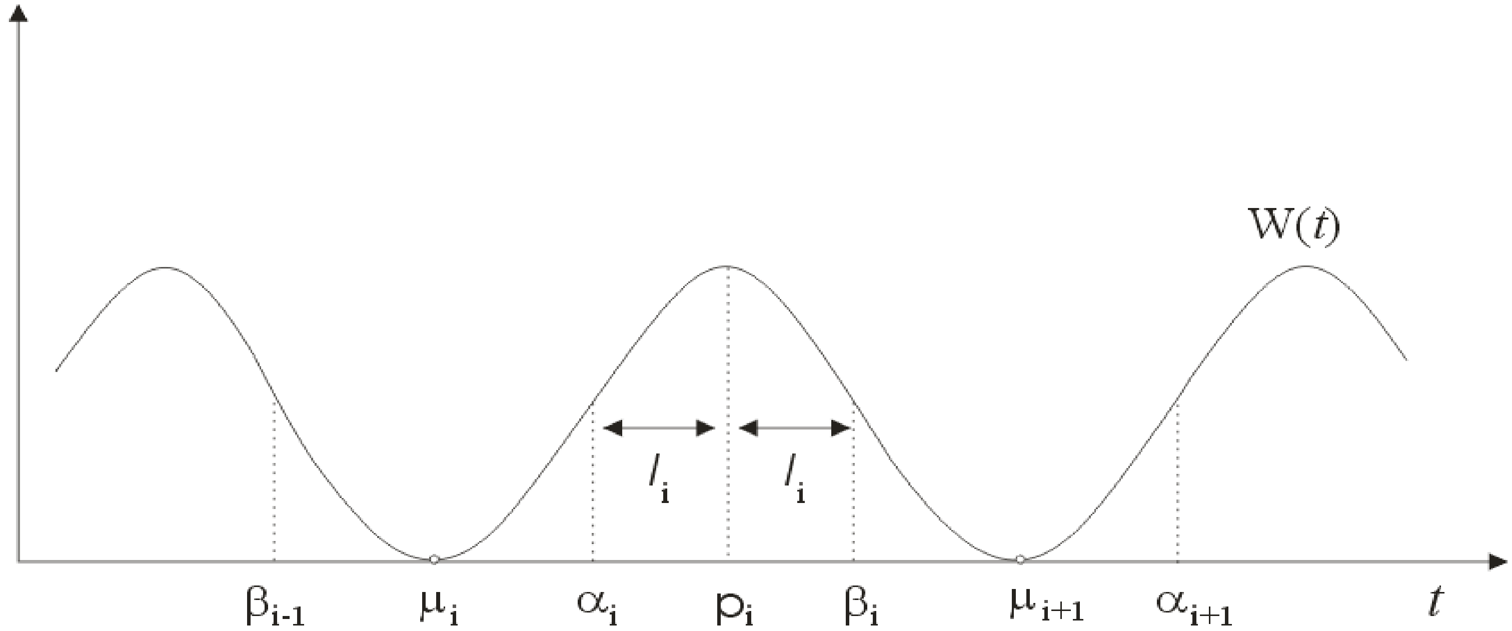

Minimization strategies

Stochastic approach
(Simulated Annealing)

Deterministic approach
(gradient based)

DISCRETE TOMOGRAPHY

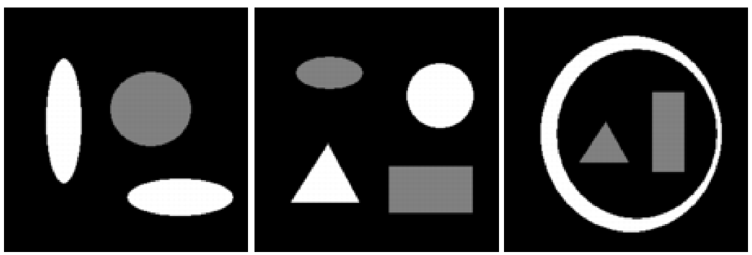

PH1 PH2 PH3

Phantom (original) images, N=256x256.
3 intensity levels,

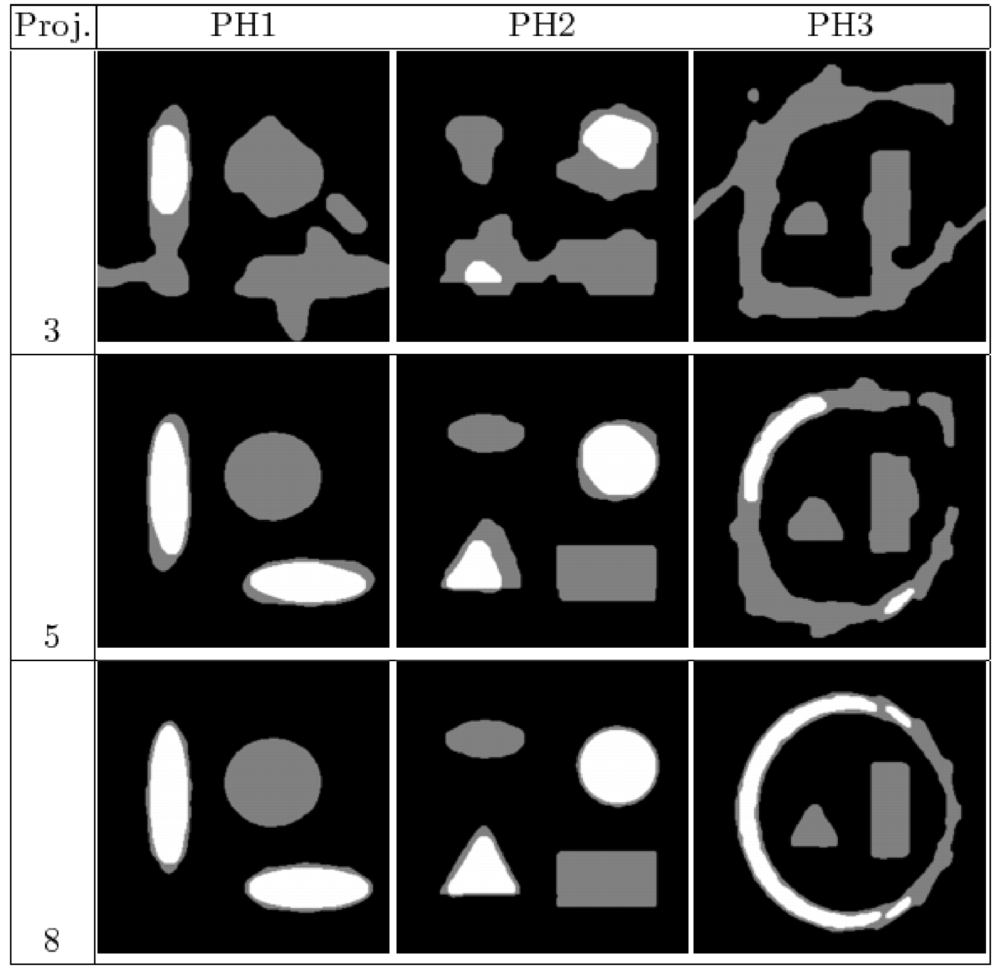

DISCRETE TOMOGRAPHY ON TRIANGULAR GRID

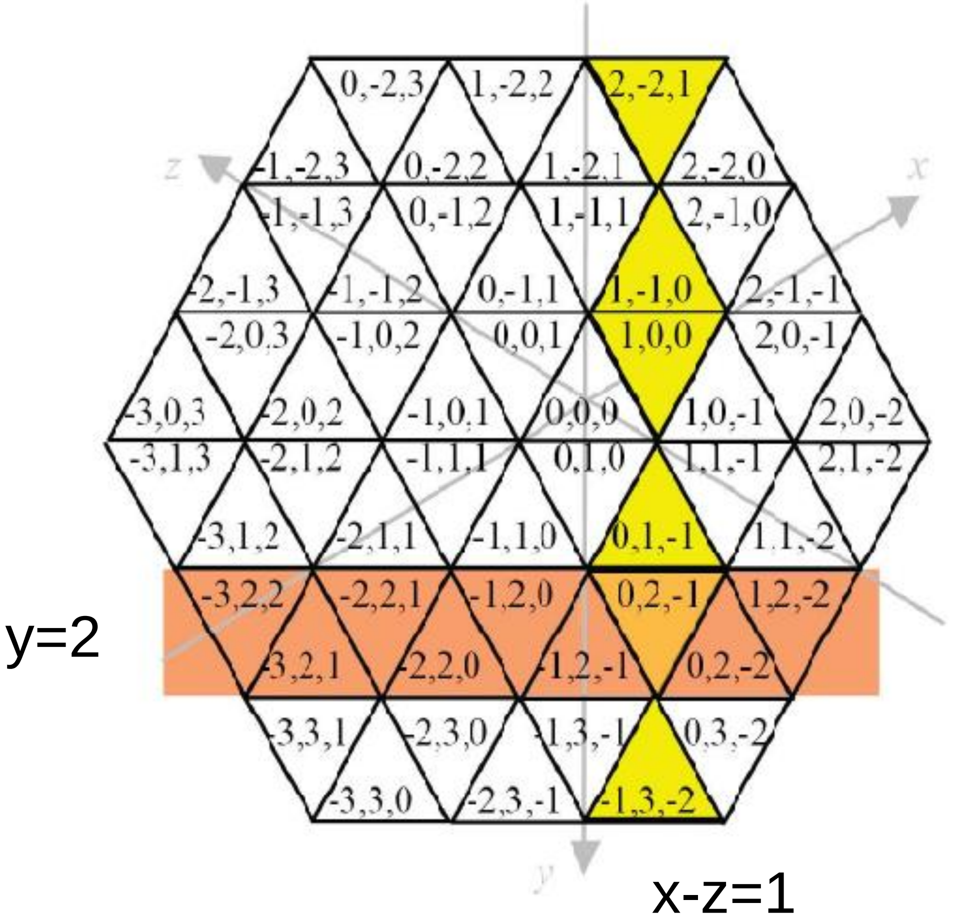

Reconstructions from

3 projections and
6 projections.

DISCRETE TOMOGRAPHY

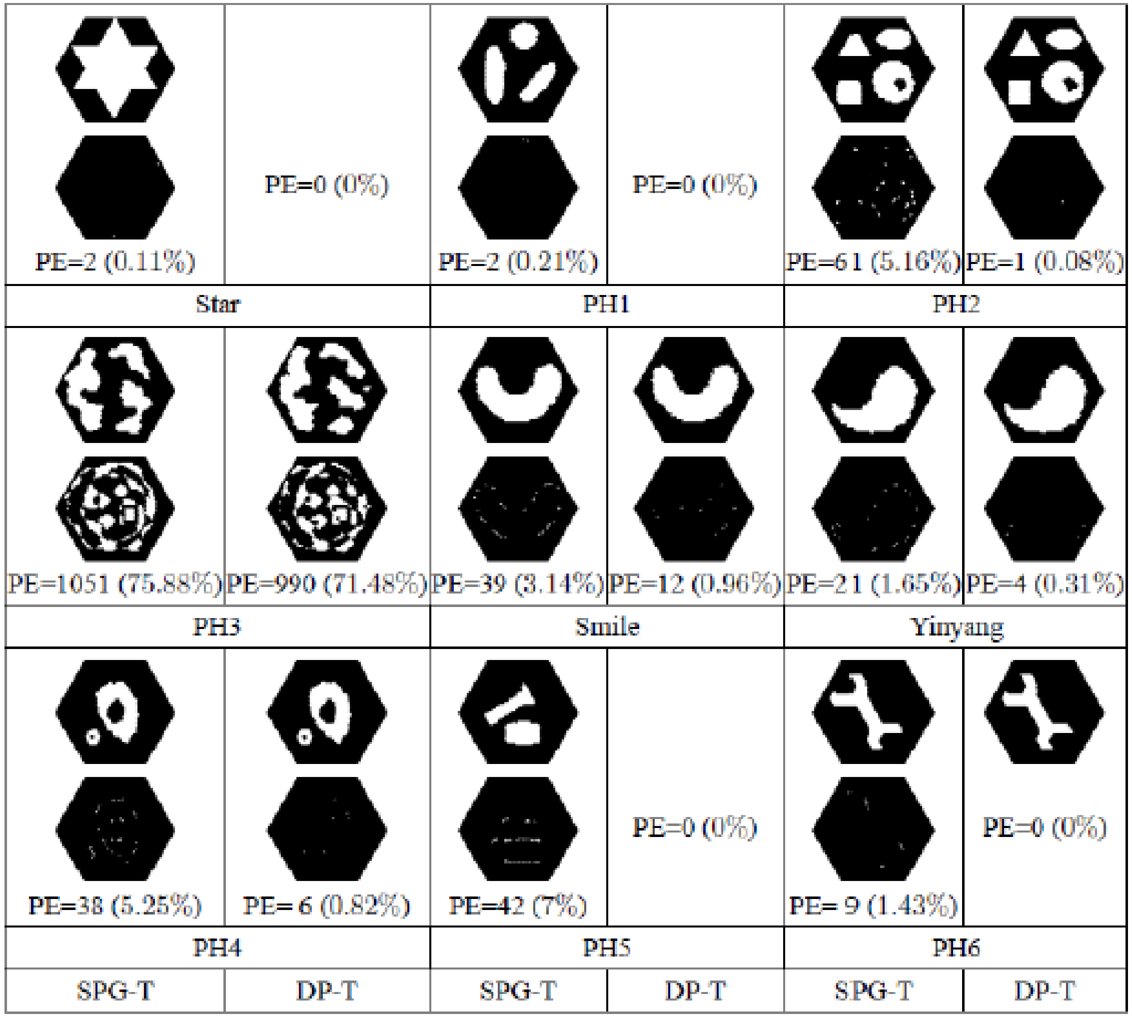

[Benedek Nagy and Tibor Lukic, Dense Projection Tomography on the Triangular Tiling, Fundamenta Informaticae, IOS Press, Vol. 145, pp. 125-141, 2016.]

REGULARIZATION

We 3always looking for new regularizations...

SHAPE DECRIPTORS ARE POSSIBLE REGULARIZATIONS.

- Elongation

- Compactness (circularity)

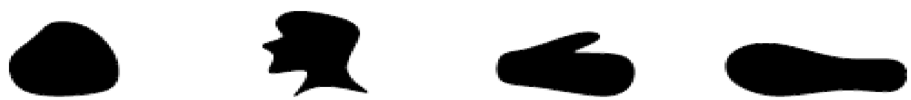

- Ellipticity

- Convexity

The shape, as an object property, allows a wide spectrum of Numerical characterizations or measures.

Basic requirements: invariance with respect to translation, Rotation, and scaling transformations.

The same numerical value should be assigned to all the shapes.

Shape measures

- Compactness/Circularity:
"Among all shapes with the same perimeter, the circle has the largest area."

$$\frac{4 \cdot \pi \cdot Area\_of\_S}{(Perimeter\_of\_S)^2}$$

"Circle minimizes the average distance of shape points to the shape centroid."

$$\frac{\mu_{0,0}(S)^2}{2\pi\left(\mu_{2,0}(S) + \mu_{0,2}(S)\right)}$$

- Convexity:

$$\frac{Area\_of\_S}{Area\_of\_CH(S)} \quad \text{but also} \quad \frac{Per\_of\_CH(S)}{Per\_of\_S}$$

Most common requirements for shape measures are:

(a) $\mathrm{D}(S) \in [0,1]$

(b) $\mathrm{D}(S) = 1$
emphif and only if S satisfies a certain property (here called a shape descriptor) for which, actually, the shape measure $\mathrm{D}(S)$ is designed.

(c) $\mathrm{D}(S)$ is invariant with respect to the similarity transformations.

(d) For any $\delta > 0$ there is a shape S such that $\mathrm{D}(S) < \delta$
(e.g., 0 is the best possible lower bound for $\mathrm{D}(S)$.)

Geometric (area) moments of order p+q:

$$m_{p,q}(S) = \iint_S x^p y^q dx\, dy.$$

The approximation is very simple to compute,
and it is very accurate:

$$m_{p,q}(S) = \iint_S x^p y^q dx\, dy \approx \sum_{\text{pixel } (i,j) \text{ belongs to } \mathrm{dig}(S)} i^p \cdot j^q$$

[R. Klette, J. Žunić, *On Discrete Moments of Unbounded Order*, LNCS **4245** (2006), 367–378.]

Moments are very desirable operators in discrete space,
because no infinitesimal process required, in opposite to gradient:

$$\nabla u(x, y) = \left(\frac{\partial u(x, y)}{\partial x}, \frac{\partial u(x, y)}{\partial y} \right)$$
$$= \left(\lim_{\Delta x \to 0} \frac{u(x + \Delta x, y) - u(x, y)}{\Delta x}, \lim_{\Delta y \to 0} \frac{u(x, y + \Delta y) - u(x, y)}{\Delta y} \right).$$

Central moments are *translation invariant*:

$$\overline{m}_{p,q}(S) = \iint_S (x - x_c(S))^p \, (y - y_c(S))^q \, dx \, dy$$

where $(x_c(S), y_c(S)) = \left(\frac{m_{1,0}(S)}{m_{0,0}(S)}, \frac{m_{0,1}(S)}{m_{0,0}(S)} \right)$ is the centroid of S.

Normalized moments are also *scaling invariant* too:

$$\mu_{p,q}(S) = \frac{\overline{m}_{p,q}(S)}{m_{0,0}(S)^{1+\frac{p+q}{2}}}$$

that is $\mu_{p,q}(S) = \mu_{p,q}(\mathbf{r} \cdot S)$.

Normalized moments are translation + scaling invariant.

Hu moments (algebraic invariants)
are also *rotational invariant*:

$$
\begin{aligned}
M_1 &= \mu_{20} + \mu_{02} \\
M_2 &= (\mu_{20} - \mu_{02})^2 + 4\mu_{11}^2 \\
M_3 &= (\mu_{30} - 3\mu_{12})^2 + 3(\mu_{21} + \mu_{03})^2 \\
M_4 &= (\mu_{30} + \mu_{12})^2 + (\mu_{21} + \mu_{03})^2 \\
M_5 &= (\mu_{30} - 3\mu_{12})(\mu_{30} + \mu_{12})[(\mu_{30} + \mu_{12})^2 - 3(\mu_{21} + \mu_{03})^2] + \\
&\quad (3\mu_{21} - \mu_{03})(\mu_{21} + \mu_{03})[3(\mu_{30} + \mu_{12})^2 - (\mu_{21} + \mu_{03})^2] \\
M_6 &= (\mu_{20} - \mu_{02})[(\mu_{30} + \mu_{12})^2 - (\mu_{21} + \mu_{03})^2] + 4\mu_{11}(\mu_{30} + \mu_{12})(\mu_{21} + \mu_{03}) \\
M_7 &= (3\mu_{21} - \mu_{03})(\mu_{30} + \mu_{12})[(\mu_{30} + \mu_{12})^2 - 3(\mu_{21} + \mu_{03})^2] + \\
&\quad (\mu_{30} - 3\mu_{12})(\mu_{21} + \mu_{03})[3(\mu_{30} + \mu_{12})^2 - (\mu_{21} + \mu_{03})^2]
\end{aligned}
$$

Hu moments are translation, scaling and rotation invariant.

Drawback: no clear “geometric” behavior.

SHAPE ORINETATION AS A REGULARIZATION

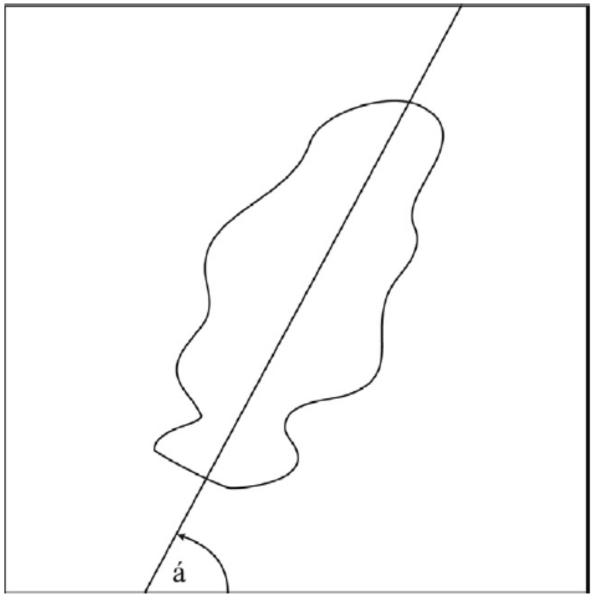

Fig. 2. Illustration of a shape and its orientation α.

The *shape orientation* is an angle alpha which satisfies the formula:

$$\frac{\sin(2\alpha)}{\cos(2\alpha)} = \frac{2 \cdot \bar{m}_{1,1}(u)}{\bar{m}_{2,0}(u) - \bar{m}_{0,2}(u)}.$$

where,

$$\bar{m}_{p,q}(u) = \sum_{(i,j)\in\Omega} u(i,j)(i - x_c)^p (j - y_c)^q$$

Of course, shape orientation is translation invariant.

SHAPE ORINETATION AS A REGULARIZATION

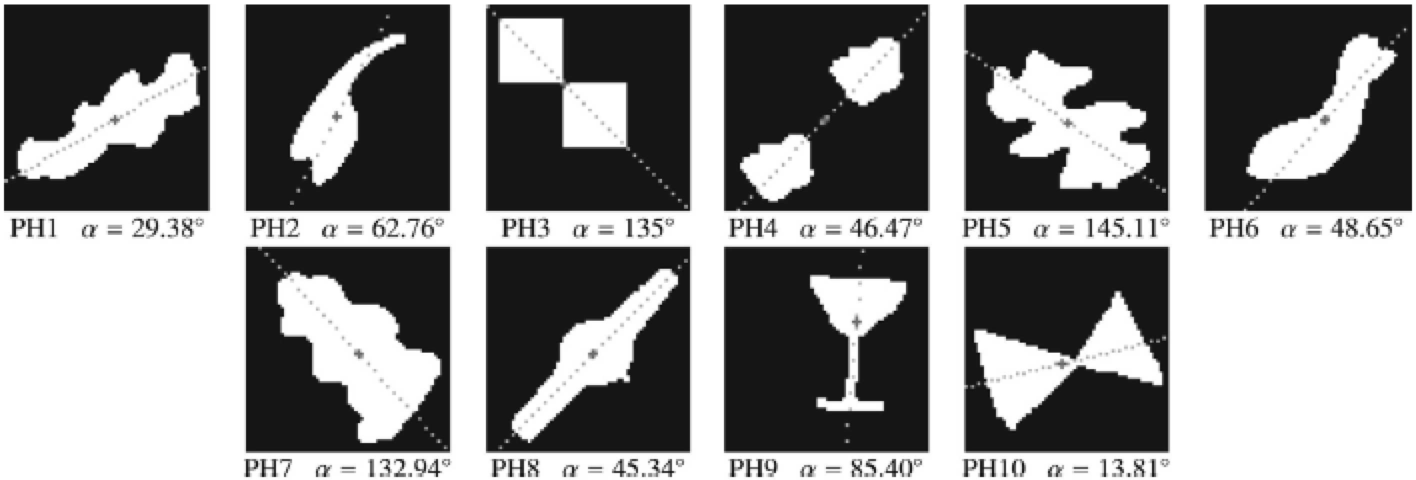

Binary images (shapes) and their orientations.

Binary tomography energy model with orientation based regularization:

$$\frac{1}{2}\left(w_P\|Au-b\|_2^2+w_H\sum_{i=1}^{N}\sum_{j\in\Upsilon(i)}(u_i-u_j)^2+w_O(\Phi(u)-\alpha^*)^2\right)$$

SHAPE ORINETATION AS A REGULARIZATION

Experimental results:

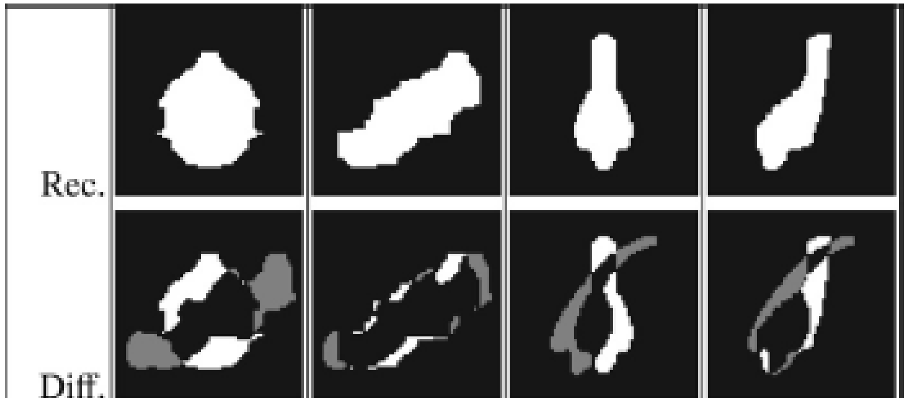

r.m.	SPG	BTO	SPG	BTO
PE/MR	811/19.79%	313/7.64%	504/12.30%	366/8.93%
PRE	7.54	3.00	5.47	2.44
$\Delta\alpha$	60.61°	5.53°	27.23°	1.26°

Fig. 8. Reconstructions of the PH1 (left two columns) and PH2 (right two columns) test images using only the horizontal projection direction.

Tibor Lukic and Peter Balazs, Binary tomography reconstruction based on shape orientation, Pattern Recognition Letters, Vol. 79, pp. 18-24, Elsevier, 2016.

SHAPE ORINETATION AS A REGULARIZATION

more experimental results:

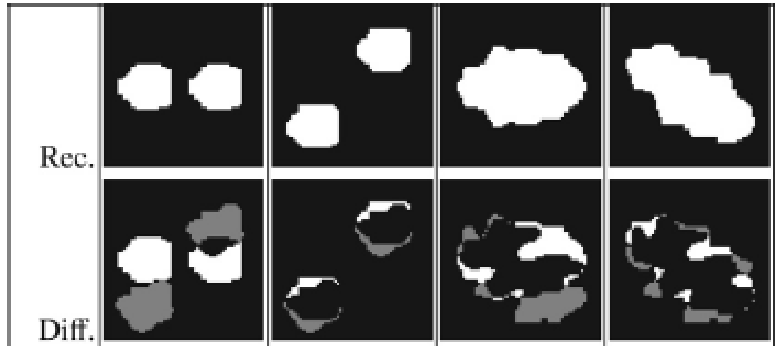

r.m.	SPG	BTO	SPG	BTO
PE/MR	1096/26.76%	242/5.91%	681/16.63%	396/9.67%
PRE	5.65	5.29	6.08	2
$\Delta\alpha$	133.39°	0.05°	144.54°	1.15°

Fig. 9. Reconstructions of the PH4 (left two columns) and PH5 (right two columns) test images using only the vertical projection direction.

Noise sensitivity:

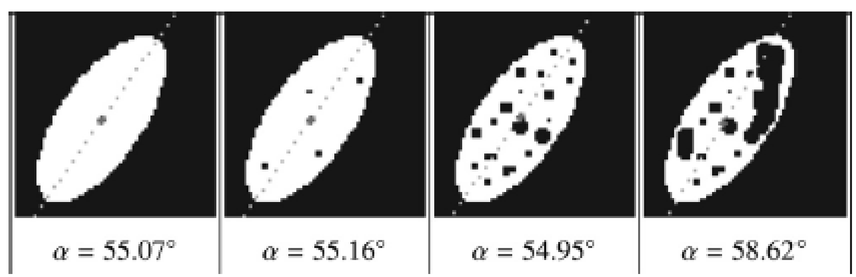

Fig. 12. Sensitivity of the shape orientation function to the degradation (caused by holes) of the object.

Elongation (ellipticity) based image denoising.

$$\mathcal{E}(u) = \frac{m_{2,0}(u) + m_{0,2}(u) + \sqrt{4\cdot\left(m_{1,1}(u)\right)^2 + \left(m_{2,0}(u) - m_{0,2}(u)\right)^2}}{m_{2,0}(u) + m_{0,2}(u) - \sqrt{4\cdot\left(m_{1,1}(u)\right)^2 + \left(m_{2,0}(u) - m_{0,2}(u)\right)^2}}.$$

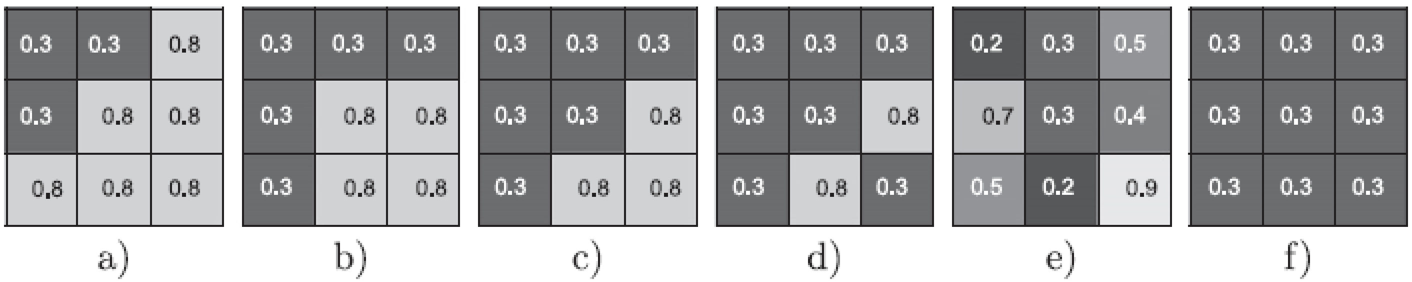

Figure 1. Calculated values of the elongation and discrete gradient magnitude. (a) $\mathcal{E}(2,2) = 1.46$, $\| \nabla u(2,2) \| = 0$; (b) $\mathcal{E}(2,2) = 1.25$, $\| \nabla u(2,2) \| = 0$; (c) $\mathcal{E}(2,2) = 1.23$, $\| \nabla u(2,2) \| = 0.71$; (d) $\mathcal{E}(2,2) = 1.06$, $\| \nabla u(2,2) \| = 0.71$; (e) $\mathcal{E}(2,2) = 1.26$, $\| \nabla u(2,2) \| = 0.14$; (f) $\mathcal{E}(2,2) = 1$, $\| \nabla u(2,2) \| = 0$. Elongation $\mathcal{E}(2,2)$, at the pixel $(2,2)$, is computed as the elongation of the 3×3 block of the surrounding pixels ((2.11) is used), while the gradient magnitude is computed by (1.7). Pixel intensities $u(x,y)$ are inscribed in the corresponding pixels.

Tibor Lukic and Jovisa Zunic, A non-gradient-based energy minimization approach to image denoising problem, Inverse Problems, Vol. 30 (095007), IOP Publishing, 2014.

SHAPE ORINETATION AS A REGULARIZATION

Instead of gradient we use the elongation operator.

$$E_{\mathcal{E}}(u) = \sum_{(i,j)\in\Omega} \mathcal{E}\left(N(i,j)\right) + \frac{\mu}{2}\sum_{(i,j)\in\Omega}\left(u(i,j) - g(i,j)\right)^2,$$

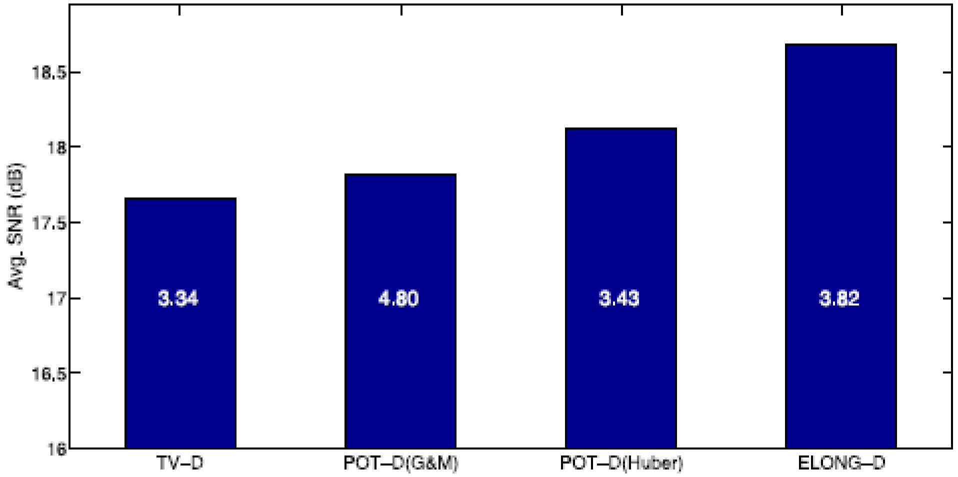

SHAPE ORINETATION AS A REGULARIZATION

Inverse Problems 30 (2014) 095007 T Lukić and J Žunić

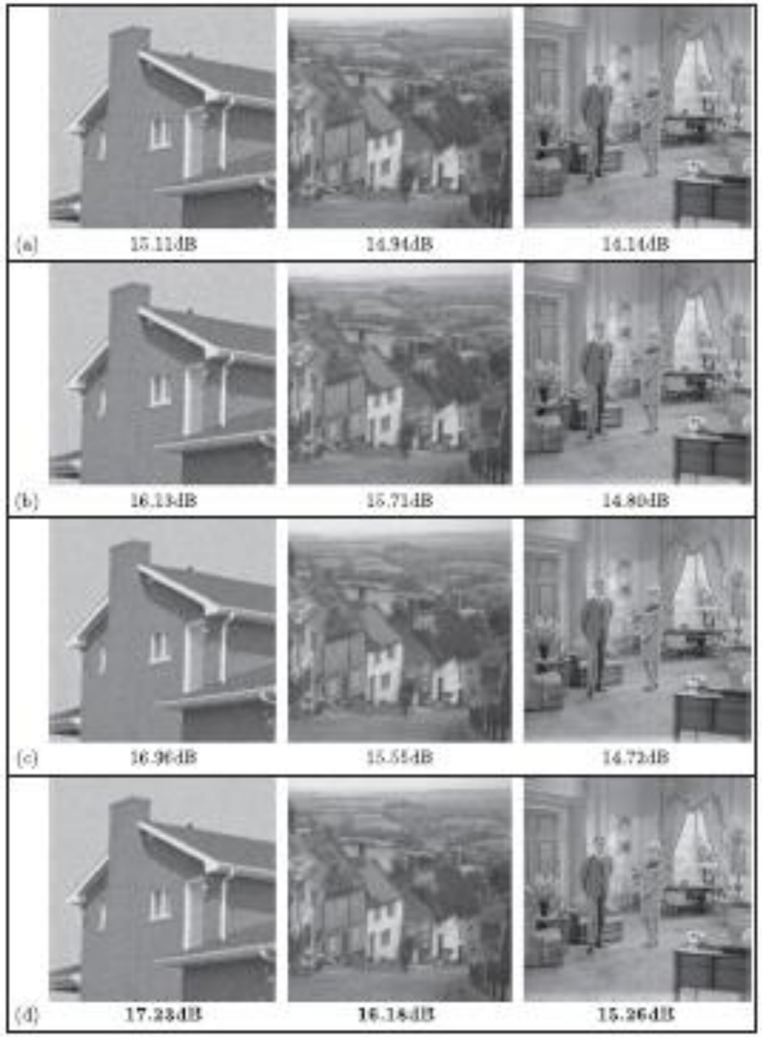

Figure 5. Reconstruction of noisy images presented in figure 3 (second row) using four different denoising methods: TV-D (a), POT-D (Huber) (b), POT-D (G&M) (c) and ELONG-D (d). The numbers below the reconstructed images show the achieved SNR values after denoising.

LITERATURE

[1] L. Armijo, *Minimization of Functions having Lipschitz Continuous First Partial Derivatives*, Pacific J. Math., 1 (1966), pp. 1–3.

[2] G. Aubert and P. Kornprobst, *Mathematical Problems in Image Processing*, Springer, 2006.

[3] Kees Joost Batenburg and Jan Sijbers, *DART: A Fast Heuristic Algebraic Reconstruction Algorithm for Discrete Tomography*, in Proceedings of International Conference on Image Processing (ICIP), 2007, pp. 133–136.

[4] E.G. Birgin, J.M. Martínez, and M. Raydan, *Nonmonotone Spectral Projected Gradient Methods on Convex Sets*, SIAM J. on Optimization, 10 (2000), pp. 1196–1211.

[5] G. T. Herman and A. Kuba, *Advances in Discrete Tomography and Its Applications*, Birkhäuser, 2006.

[6] T. Lukić, J. Lindbald, and N. Sladoje, *Regularized Image Denoising Based on Spectral Gradient Optimization*, Inverse Problems, 27 (2011), p. 17 pp.

[7] T. Lukić and J. Žunić, *A non-gradient-based energy minimization approach to the image denoising problem*, Inverse Problems, 30 (2014), p. 19 pp.

[8] J. Nocedal and S. J. Wright, *Numerical Optimization*, Springer, 2006.

[9] Natasa Sladoje, Joakim Lindblad, and Ingela Nyström, *Defuzzification of Spatial Fuzzy Sets by Feature Distance Minimization*, Image Vision Comput., 29 (2011), pp. 127–141.

[10] M. Zhu and T. Chan, *An Efficient Primal-Dual Hybrid Gradient Algorithm For Total Variation Image Restoration*, UCLA CAM Report, (2008), pp. 08–34.

THANK YOU FOR YOUR ATTENTION!